Development of a High-Resolution Shallow Seismic Refraction Tomography System at the Monterey Bay Aquarium Research Institute

R. Henthorn[1], D. W. Caress[1], M. R. Chaffey[1], P. R. McGill[1], W. J. Kirkwood[1], C. K. Paull[1], W. C. Burgess[2]

1. Monterey Bay Aquarium Research Institute, Moss Landing, CA, USA.

2. Greeneridge Sciences, Santa Barbara, CA, USA.

Fall AGU 2009

OS21A-1148

The Problem: Resolving the Subsurface Structure of Marine Methane Hydrate Deposits

For several years, the Monterey Bay Aquarium Research Institute has devoted considerable effort to the study of the geological and geochemical processes associated with the formation and dissociation of methane hydrate deposits (e.g. Brewer et al., 2002; Hester et al., 2007a,b; Naehr et al., 2000; Paull, 2002; Paull et al., 2003, 2005, 2007, 2008; Peltzer and Brewer, 2000, Ussler and Paull, 2001). These projects have made use of a combination of ROV-based exploration, sampling, in situ analyses (e.g. laser raman spectroscopy), seismic reflection profiling, and AUV-based high resolution seafloor mapping and subbottom imaging (Paull et al., 2008; Caress et al., 2008). However, MBARI's ability to investigate the mechanisms for formation of massive hydrate exposures have been limited by an inability to resolve the subsurface structure of these deposits. Although AUV-mounted chirp subbottom profiler sonars can achieve penetrations of 50 m or more in soft, well stratified sediments, these systems tend to poorly image the subsurface where hydrates are present because the high sound velocity hydrates and/or authigenic carbonates mask the pre-existing sedimentary features. Also, gas bubbles, when present, highly attenuate the acoustic signals, thereby contributing to blank zones in seismic reflection and subbottom profiler sections. The figures below present results from ROV dives and a Mapping AUV survey of gas seep mounds in Santa Monica Basin (Paull et al., 2008); these data fail to unequivocally discriminate between plausible models for the formations of these mounds. Observations constraining the shallow subsurface distribution of hydrates at a resolution of a few meters are required.

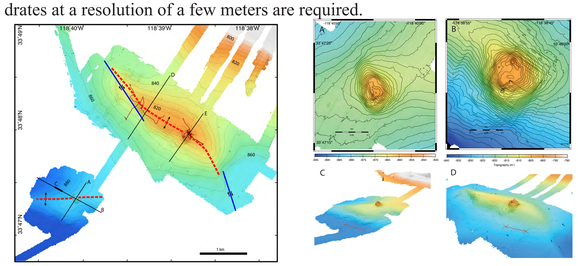

Results from Mapping AUV survey and ROV dives on Santa Monica gas seep mounds (Paull et al., 2008).
(Top left) Bathymetric maps generated by AUV multibeam surveys across the NE and SW Mounds and Swells shown at 5 m contour interval. Location of chirp seismic profile sections illustrated in A-E are indicated (black lines). Locations of ROV dives (thin red lines), the axial trace of the anticline (red dashed line) and inferred strike slip faults (blue line) are also indicated.
(Top right) 1 m contour maps and perspective views of the Santa Monica mounds. (Right) High-resolution seismic reflection profiles of the Santa Monica Mounds and swells collected using the chirp system on MBARI's mapping AUV.
Profile A extends NE-SW across the SW Mound and illustrates that this topographic high is associated with an anticline. Profile B extends NW-SE along the crest of the swell and crosses the SW Mound. The reflection profile does not resolve internal structure of the mound. Profile C is an expanded view of part of profile B and shows several small normal faults (F) on its NW limb. Profile D shows a crossing of the NE Swell and shows faulting (F) on its southwest limb. Profile E crosses the NE Mound.

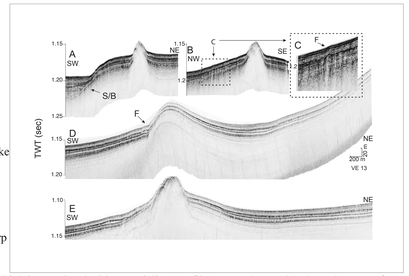

(Left) Video images collected during dives of the ROV Tiburon showing the seafloor on the NE Santa Monica Mound and photographs of samples collected from the NE Mound. Part A shows a crack near the crest of the mound from which a continuous plume of gas emanates. Bubbles can be seen above the ROV's manipulator. The manipulator is holding an overturned cylinder with an attached funnel to collect the gas. The white material in the cylinder is a mush of gas-hydrate-coated bubbles. Cylinder is 9 cm in diameter. Part B shows the contact between a white-fringed patch of orange microbial mat and a bed of living clams on a terrace on the southwestern flank of the mound. Part C shows a densely packed bed of V. elongata. Part D shows a cross section of authigenic carbonate rock. Articulated valves of V. elongata shells are contained within this sample. A 2.5-cm long V. elongata shell found nearby is shown for scale. It also provides a coarse scale for the images in Parts B and C.

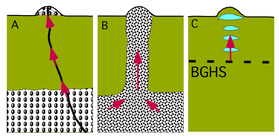

(Right) Cartoon showing the three possible mechanisms for producing seafloor mounds. Part A represents a mud volcano where the topography is composed of reconstituted material extruded as a slurry from the subsurface. Part B represents a diapir where the solids have flowed upward and deform the seafloor. Part C illustrates the effect of expansion associated with the growth and accumulation of gas hydrate in the subsurface. Paull et al. (2008) prefer C, but the existing data do not conclsively distinguish between these models.

The Concept: High-Resolution Seismic Refraction using Seafloor Hydrophones and an Acoustic Chirp Source

One approach to imaging subsurface hydrate distribution is seismic refraction, in which seismic sources and receivers are separated so that arrivals reflect energy that has propogated laterally through the subsurface. The refraction technique is attractive because "hydrated" sediments have a significantly higher compressional seismic velocity than water-saturated sediments (e.g. Lee et al., 1996), as do authigenic carbonates associated with methane-related diagenesis. Refraction experiments typically combine seismometers or hydrophones deployed on the seafloor with pneumatic sound sources (airguns), or similar devices, operated at the sea surface from ships. However, in order to achieve the desired resolution, both sources and receivers must be located on or near the seafloor. Although discrete explosive and implosive sources (e.g. Christensen et al., 1992; Hammer et al., 1994) have been used in deep-ocean on-bottom refraction experiments, sources that are more repeatable, easier to generate, and higher in frequency (on the order of 1-5 kHz rather than 1-100 Hz) are needed. Subbottom profiler sonars generate highly repeatable acoustic signals at depth, and can use long duration swept-frequency (chirp) source functions to improve both the signal-to-noise ratio and time-resolution of arrivals. In addition, to make experiments logistically feasible, the receivers should be easily deployable in precise locations and the source must be capable of being operated continuously along profiles on or near the seafloor.

The cartoon illustrates our initial concept for an ROV-based, deep-ocean, high resolution seismic refraction system. The acoustic source is an ROV-mounted sonar producing a 1-6 kHz chirp signal, and the receivers are small hydrophone recording packages. Operationally we deploy a number of small hydrophone recording systems on the seafloor from the ROV, run the refraction profiles along the bottom with the vehicle, and the recover the instruments.

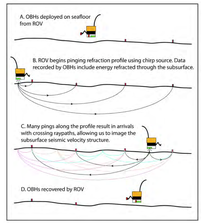

Initial Test Results

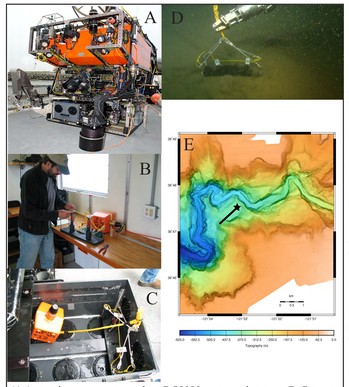

A) Acoustic source mounted on ROV Ventana swing arm. B. Preparing hydrophones for deployment - when on the seafloor the hydrophones are pushed into the sediment through holes in a steel plate by elastic cord under tension. C) Hydrophone assembly in ROV drawer with attached float/beacon. D) Deploying hydrophone assembly on seafloor. E) Location figure. The Hydrophones were deployed at 382 m depth on a bench above the inner canyon axis (site indicated by star), and the refraction profiles where shot along a 1 km line to the southwest.

On September 22, 2009, the ROV-based chirp refraction concept was tested from R/V Point Lobos using ROV Ventana, the 1-6 kHz chirp source described above, and two Acousonde hydrophones. The test site was in about 380 m of water in the upper Monterey Canyon. Initially, the hydrophones were lowered to 110 m depth and the ROV brought to within 30 m range so that the actual source pulses achieved could be recorded without interference from reflections. Then the hydrophones were deployed on the seafloor at 382 m on a bench south of the canyon axis, and Ventana ran four 1 km long refraction profiles along the bottom pinging at 3 second intervals using tapered 0.25-6 kHz chirps with 25, 50, 100 and 200 millisecond pulse durations, respectively. Similar results where achieved with all four pulses; the 25 millisecond case is displayed to the right. The match filtering was applied using the actual rather than modeled sources. The raw wavefield data is dominated by noise from the ROV and ship. The match filtering succeeds admirably in resolving the direct and surface reflected arrivals, but no refracted arrivals are observed. The noise analysis below suggests that the ROV is simply too noisy for low amplitude refractions to be observed. A less noisy source platform will be required for an acoustic chirp refraction system to work.

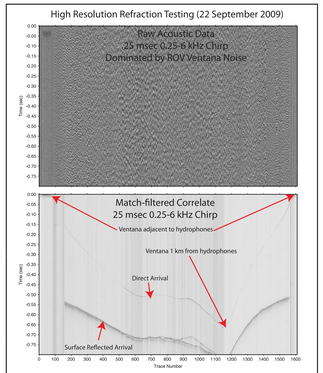

Example of test refraction data using a 25 millisecond chirp. (Top) Raw wavefield recorded by hydrophones. This is dominated by a combination of ROV and ship acoustic noise. (Bottom) Result of match filtering, or "dechirping" the hydrophone data. The direct and surface bounced arrivals are resolved as expected, but no refracted arrivals are observed.

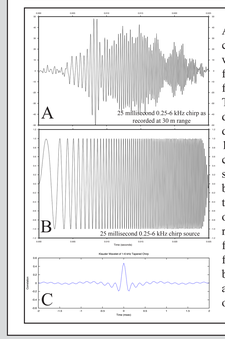

A) 25 millisecond 0.25-6 kHz chirp as recorded in midwater at 30 m range. The midwater tests allowed the achieved source function to be recorded without interference from seafloor and seasurface reflections. The frequency sweep started at 0.25 kHz to determine if the source transducer can be driven below its rated frequency range of 1-6 kHz. B) 25 millisecond 0.25-6 kHz chirp source function. Note that actual source achieved in (A) has little energy below 1 kHz. In the future the source functions will run 1-6 kHz. (C) Klauder wavelet obtained as the autocorrelation of (B). This represents the idealized impulse response function obtained by "dechirping" (match filtering) the recorded acoustic data. The best possible time resolution of an arrival after match filtering is about 0.25 milliseconds.

Spectrograms of hydrophone data formed by calculating power spectra as a function of time. (Left) Spectrogram for hydrophones hung in midwater near the ROV. The acoustic noise generated by ROV Ventana is obvious. Noise reduction observed when the vehicle hydraulics are turned off verifies that the hydraulic pump and associated vibration are a large source of noise. Interestingly, the ROV noise is apparently dominated by harmonics of 565 Hz extending to nearly 10 kHz. (Right) Spectrogram from hydrophones deployed on seafloor as refraction profiles were run using 25, 50, 100, and 200 millisecond 0.25-6 kHz chirp pulses.The hydrophones were saturated by ship and ROV noise during deployment, recovery, and when the ROV approached closely at the start and ends of the profiles.

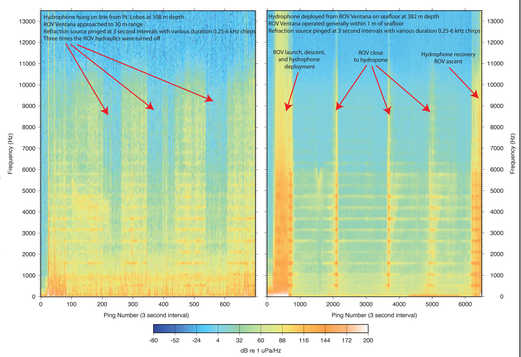

Hydrophone Recording System

The hydrophone package is an Acousonde miniature autonomous acoustic recorder recently developed with ONR funding by Acoustimetrics, part of Greeneridge Sciences, Inc. The primary purpose of this instrument is marine mammal monitoring. Specifications relevant to the refraction application include:

- 26 kHz sampling rate
- 10 Hz to 9.2 kHz bandwidth
- 16 bit sampling
- 8 GB flash storage
- 42 hour recording duration
- 6-pole elliptic anti-aliasing filter
- 167 dB re 1 uPa saturation at 20 dB gain setting
- 3000 m depth rating

A combination of internal clock discipline, and post-deployment calibration achieves timing accuracy well within the 250 microsecond theoretical resolution of refracted arrival travel times.

1-6 kHz Chirp Acoustic Source

The ROV-mounted acoustic source consists of the amplifier and projector for an Edgetech 1-6 kHz subbottom sonar driven by a National Instruments cRIO realtime controller and LabView software. This architecture allows us to test a wide variety of source waveforms. The projector is shown at right mounted to the swing arm of ROV Ventana. The source strength is approximately 206 dB re 1 uPa at 1 m range.

Acoustic Noise Measurements of the MBARI Mapping AUV

In order to test the suitability of Dorado AUVs as refraction source platforms, we deployed two Acousonde hydrophones on the seafloor at a depth of 110 m in the path of the MBARI Mapping AUV during a seafloor mapping survey. The AUV ran at a 50 m altitude at 1.5 m/sec, pinging a subbottom profiler every 0.5 seconds with a 2-10 kHz, 20 msec chirp pulse. The sonogram at right shows that the acoustic noise generated by the AUV has peaks of about 70 dB at 1.2 kHz and 1.8 kHz, with negligible noise above 2 kHz. The subbottom profiler signal appears strongest in the sonogram at 300 m range, presumably due to reverberation in the water column. Clearly the AUV is a quieter and therefore better platform for the refraction acoustic source. We are currently upgrading the Mapping AUV subbottom profiler to use the 1-6 kHz source, and **future refraction tests will use the AUV as the acoustic source platform.**

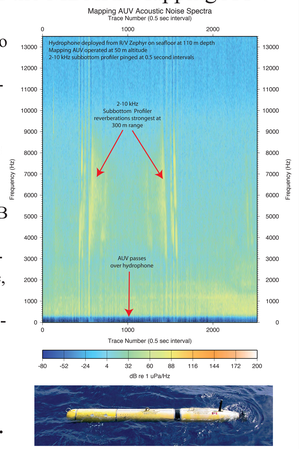

2010 High-Resolution Refraction Experiment at the Northern Santa Monica Gas Seep Mound

The next phase of the MBARI high-resolution refraction project will be a test at the northern Santa Monica gas seep mound in the spring of 2010. This experiment is intended to compare the seismic velocity structure of the upper 100 m beneath the crest of the mound, from which free methane escapes, with that beneath the seafloor north of the mound, where no evidence for subsurface gas or hydrate exists. Five hydrophones will be deployed along a 1.5 km long profile along the crest (shown on the map) using the ROV Doc Ricketts on R/V Western Flyer, and then the Mapping AUV (deployed from R/V Zephyr) will fly the profile at a 10 m altitude, pinging the 1-6 kHz source at 3 second intervals. The ROV will be used to move the instruments to a second profile located 500 m to the northwest, and then the AUV will run a second refraction profile. In addition to using the quieter AUV as the source platform, the likelihood of success will be augmented by using a new version of the Acousonde hydrophone with an additional 10 dB of preamplifier gain.

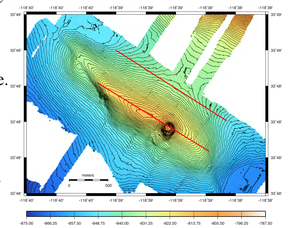

R/V Zephyr deploying Mapping AUV

R/V Western Flyer (equipped with ROV Doc Ricketts)

References

Brewer, P.G., C.K. Paull, E.T. Peltzer, W. Ussler, III, G. Rehder, and G.E. Friederich (2002). Measurements of the fate of gas hydrates during transit through the ocean water column. Geophysical Research Letters, 29: doi10.1029/2002GL014727.

Caress, D.W., H. Thomas, W.J. Kirkwood, R. McEwen, R. Henthorn, D.A. Clague, C.K. Paull, J.B. Paduan, and K.L. Maier (2008). High-resolution multibeam, sidescan, and subbottom surveys of seamounts, submarine canyons, deep-sea fan channels, and gas seeps using the MBARI AUV D. Allan B. In: Marine Habitat Mapping Technology for Alaska, edited by J.R. Reynolds and H.G. Greene. Alaska Sea Grant College Program, University of Alaska Fairbanks, pp. 47-70.

Christeson, G. L.; Purdy, G. M.; Fryer, G. J. (1992), Structure of young upper crust at the East Pacific Rise near 9 deg 30 N, Geophysical Research Letters (ISSN 0094-8276), 19, 1045-1048.

Hammer, P. T. C., L. M. Dorman, J. A. Hildebrand, and B. D. Cornuelle (1994), Jasper Seamount structure: Seafloor seismic refraction tomography, J. Geophys. Res., 99(B4), 6731–6752.

Hester, K.C., R.M. Dunk, P. Walz, E.T. Peltzer, E.D. Sloan, and P.G. Brewer (2007). Direct measurements of multi-component hydrates on the seafloor: Pathways to growth. Fluid Phase Equilibria, 261: 396-406.

Hester, K.C., R.M. Dunk, S.N. White, P.G. Brewer, E.T. Peltzer, and E.D. Sloan (2007). Gas hydrate measurements at Hydrate Ridge using Raman spectroscopy. Geochimica et Cosmochimica Acta, 71: 2947-2959.

Lee, M.W., Hutchinson, D.R., Agena, W.F., Dillon, W.P., Miller, J.J. and Swift, B.A., Seismic character of gas hydrates on the southeastern U.S. continental margin, Marine Geophys. Researches, 16, 163-184, 1994.

Naehr, T.H., N.M. Rodrigues, G. Bohrmann, and C.K. Paull (2000). Methane derived authigenic carbonates associated with gas hydrates decomposition and fluid venting above the Blake Ridge Diapir. In: Proceedings of the Ocean Drilling Program, Scientific Results, edited by R. Matsumoto, Paull, C.K., and Wallace, P. 164: 285-300.

Paull, C.K. (2002). Continental margin gas hydrate: Slope stability, geo-hazard, and climate connections; Onshore-offshore relationships on the Nordic Atlantic margin. In: Proceedings of the Norwegian Geological Society. 2: 158–161.

Paull, C.K., P.G. Brewer, W. Ussler, III, E.T. Peltzer, G. Rehder, and D.A. Clague (2003). An experiment demonstrating that marine slumping is a mechanism to transfer methane from seafloor gas-hydrate deposits into the upper ocean and atmosphere. Geo-Marine Letters, 22: 198–203.

Paull, C.K., W. Ussler III, T. Lorenson, W. Winters, and J. Dougherty (2005). Geochemical constraints on the distribution of gas hydrates in the Gulf of Mexico. Geo-Marine Letters, 25: 273-280.

Paull, C.K., W. Ussler III, S. Dallimore, S. Blasco, T. Lorenson, H. Melling, F. McLaughlin, and F.M. Nixon (2007). Origin of pingo-like features on the Beaufort Sea shelf and their possible relationship to decomposing methane gas hydrates. Geophysical Research Letters, 34: doi: 10.1029/2006GL027977.

Paull, C.K., Normark, W.R., Ussler III, W., Caress, D.W., Keaten, R., "Association among active seafloor deformation, mound formation, and gas hydrate growth and accumulation within the seafloor of the Santa Monica Basin, offshore California", Marine Geology, 250, 258-275, 2008.

Peltzer, E.T. and P.G. Brewer (2000). Practical physical chemistry and empirical predictions of methane hydrate stability. In: Natural Gas Hydrate in Oceanic and Permfrost Environments, edited by M. D. Max. Kluwer Academic Publishers, Dordrecht, The Netherlands, pp. 17-28.

Ussler III, W. and C.K. Paull (2001). Ion exclusion associated with marine gas hydrate deposits. In: Natural gas hydrates: Occurrence, distribution, and detection, edited by C.K. Paull and W.P. Dillon. Washington, D.C., American Geophysical Union. 124: 41-51.